[redacted]

Magnetohydrodynamic EMP (U)

NEAL J. CARRON AND CONRAD L. LONGMIRE

Mission Research Corporation, Santa Barbara, California

(Received March 30, 1984)

(U) This paper reviews the mechanisms by which bomb-induced hydrodynamic motions in the ionosphere interact with the geomagnetic field to produce the magnetohydrodynamic EMP. Experimental data from the 1962 Starfish event are presented, and the electric fields in the ground that would result from a similar event over the northern United States are calculated. The maximization of this phenomenon by optimum choice of burst parameters is discussed briefly, along with the possible effects on long-haul telephone lines and the electric power grid.

I. INTRODUCTION

(U) Nuclear explosions at high altitude produce strong hydrodynamic motions over large volumes of space. For example, while a 1-Mt burst at sea level produces a shock wave that is ionizing out to distances of the order of 1 km, the same burst at 400-km altitude makes shock-induced ionization to distances of several hundred kilometers. When the shock wave is conducting, the expanding air (and bomb debris) tends to carry the geomagnetic field with it. Hence explosions at high altitudes can put significant fractions of the yield into distorting the geomagnetic field. For bursts at 1,000 km or higher altitudes, most of the debris kinetic energy—typically one fourth of the total yield—is expected to go into geomagnetic distortions. The time-varying magnetic field implies the existence of electric fields. These fields are generally weaker but longer lasting than the gamma-induced electromagnetic pulse (EMP) and are important for long-wire systems such as power transmission lines and long haul telephone lines.

(U) The generation of the magnetohydrodynamic (MHD) EMP involves varied and complicated mechanisms, but it appears that two principal mechanisms are dominant.

II. THE MHD SHOCK WAVE EFFECT

(U) The shock wave is the first hydrodynamic signal to arrive at observer points away from the burst point. At high altitude, the shock wave is driven by just the debris kinetic energy, since the x-ray energy (typically 70 percent of yield) is not absorbed appreciably near the burst point. (X-rays coming downward are absorbed by the air typically between altitudes of 60 to 100 km.) The speed of the shock wave is initially set by the debris speed, of the order of 2,000 km/sec, but cannot be less than the local magnetosonic speed. As more air mass is swept up, the shock speed decreases to the magnetosonic speed. At altitudes above about 150 km, only the charged particles and the magnetic field are involved in magnetosonic waves, and the speed of these waves is the Alfvén speed $B/\sqrt{4\pi\rho}$ (cgs Gaussian units: B in gauss, ρ is charged particle mass density in grams per cubic centimeter); collisions with neutral particles are too infrequent to involve the neutrals hydrodynamically.

(U) The charged particles are those preexisting in the ionosphere plus those created by the explosion. The latter include ion pairs created by absorption of the low-energy tail of the x-ray spectrum, by electron and ion impact, and by charge exchange on neutral par-

[redacted]

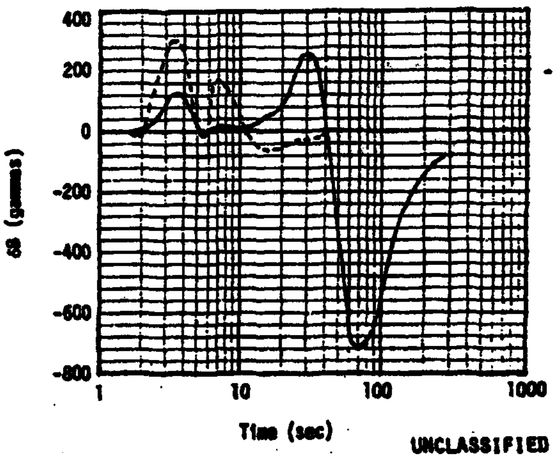

Figure 1. (U) Changes in geomagnetic intensity observed in Starfish. Solid curve is Dyal's data(²) from Johnston Island. Dashed curve is data of Bomke et al.(³) from Hawaii. Note: 1 gamma = 10^{-5} gauss.

UNCLASSIFIED

ticles. Inclusion of these processes and the tensor character of the magnetic stress results in fairly complicated calculations. Only a simplistic description is presented in this paper.(¹)

(U) The Alfvén speed v_A has a minimum at the peak of the ionospheric F-region (approximately 300-km altitude) and is about 200 km/sec daytime, 500 km/sec nighttime. At higher altitudes v_A increases; at 1,000 km it is about [redacted] km/sec daytime, 6,000 km/sec nighttime. The speeds are higher in periods of low solar activity. The increase in v_A with altitude has the result that magnetosonic rays curve downward toward the earth; the shock wave at higher altitude outruns that at lower altitude. The radius of curvature of the magnetosonic rays is of the order of 500 km. The result is that, for bursts between 400 and 1,000 km altitude, a downward-going shock wave reaches the bottom of the F-region (approximately 150 km) almost simultaneously ($\delta t < 1$ sec) over a large geographical region a few seconds after the burst, as is seen in the experimental data (Section IV).

(U) In the ionospheric E-region (100 to 150 km), collisions of ions with neutrals cause damping of the shock wave. The plasma physics of this effect is much debated, the debate centering on which of the many possible plasma resistivities (including anomalous) is operative. It seems to be generally agreed that magnetic perturbations that manage to get through the E-region then reach the ground unhindered.

III. THE ATMOSPHERIC HEAVE EFFECT

(U) The air heated by the shock wave contains a considerable fraction of the kinetic energy yield as thermal energy. These energetic, ionized particles flow along the geomagnetic field lines, both northward and southward, until they reach the E-region, where they transfer their energy by collisions to the ambient air. The heated air in these magnetic conjugate regions then expands and rises buoyantly. Rising across the geomagnetic field generates an east-west electromotive force, which drives opposite electron currents along the east and west sides of the magnetic flux tube. These currents close in the ionospheric D- and E-regions through electron and ion collisions with neutrals. The current loops make magnetic perturbations, which may be observed at ground level and which last for hundreds of seconds.

IV. EXPERIMENTAL DATA

(U) The Starfish event—about 1 megaton (Mt) at 400 km over Johnston Island at 11:00 p.m. local time July 9, 1962—caused geomagnetic perturbations that were observed worldwide. Figure 1 shows changes in magnetic intensity that were observed on Johnston Island and in Hawaii (approximately 1,300 km away from burst). We identify the positive (increased intensity) pulses occurring before 10 seconds as due to the MHD shock wave, the changes after 10 seconds as due to the heave effect. On Johnston Island, the latter

[redacted]

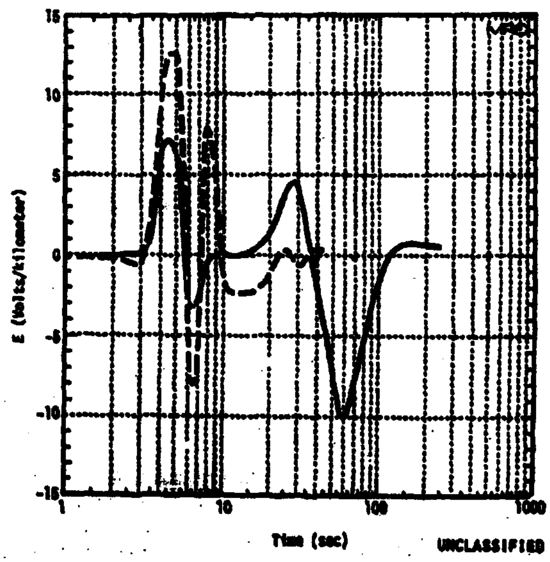

UNCLASSIFIED

Figure 2. (U) Electric fields inferred for a hypothetical Starfish event fired over the northern United States. Solid curve, underneath burst: dashed curve, 1,500 km away.

is first an increase in intensity, followed by a decrease. The change in sign is thought to come from changing position of the current loop as the heave proceeds.

(U) Note that the MHD shock effect is larger at Hawaii than at Johnston Island. This is attributed to increased E-region damping caused by x-ray-induced ionization over Johnston Island.

V. ELECTRIC FIELD IN GROUND

(U) If one tries to push a magnetic field into the conducting ground, inductive electric fields arise which drive currents in the ground, tending to oppose the change in magnetic field. The solution to the problem is governed by a diffusion type of equation and is the well-known skin effect. The skin depth at 1 second in ocean ($\sigma \sim 4$ mho/m) is 0.6 km and in soil ($\sigma \sim 10^{-3}$ mho/m) is 40 km. For other times t and σ's, the skin depth is proportional to $\sqrt{t/\sigma}$. The currents opposing the magnetic perturbations flow in this layer, from which it can be estimated that a change ΔB (gauss) occurring in time Δt (sec) causes an electric field E in the ground of magnitude

$$E(V/km) \sim 60\ \Delta B/\sqrt{\sigma \Delta t} \quad (\sigma \text{ in mho/m}) \quad (1)$$

An accurate equation relating E and B at the ground surface is (mks units)

$$E(t) = \frac{1}{\sqrt{\pi\mu\sigma}} \int_0^t \frac{1}{\sqrt{t-t'}} \frac{\partial B}{\partial t'}\, dt' \quad (2)$$

(U) If the Starfish event had occurred over the northern United States, the magnetic perturbations would have been about twice as large as those observed on the actual event, because of the larger geomagnetic field over the northern United States. Taking this factor of 2 in magnetic amplitude and assuming an average soil conductivity of 10^{-3} mho/m, our colleagues J. Gilbert and N. Goldman have used Eq. (2) to determine the electric field at the ground for this hypothetical case. The results are shown in Fig. 2 (the plot there is delayed by 1 second relative to Fig. 1). It can be seen that the peak electric field under the burst (corresponding to the Johnston Island measurements) is about 10 V/km, while the peak electric field at a distance 1,500 km away from the burst (corresponding to the Hawaii measurements) is about 13 V/km.

(U) The direction of the electric field tends to be orthogonal to the change in magnetic field. For vertical initial geomagnetic field, the electric field

[redacted]

lines are concentric circles about ground zero. For a tipped geomagnetic field, the electric field lines are, crudely, circles (nonconcentric) about two null points north and south of the burst.

VI. MAXIMIZATION OF THE MHD EMP

[redacted]

DTRA 3.3(b)(2)(8)

OSD 3.3(b)(8)

VII. EFFECTS OF MHD EMP ON SYSTEMS

(U) Electric power and telephone systems are generally grounded, to reduce personnel and equipment hazards and sometimes to use the ground as a return path for current. In the presence of the MHD EMP, a long wire grounded at one end will show either a large voltage to ground at the other end, if it is open to ground there, or a large current if it is grounded there. Both cases occur in practice. Long-haul telephone lines are designed to turn themselves off if ground potentials exceed certain limits. Electric transmission lines generally have the neutral terminal grounded at both ends. The MHD EMP then causes an essentially d.c. current to flow from the ground at one end, through the high voltage side of the transformer windings, along all three of the phase wires, through the transformers to ground at the other end. Currents in the ground connections are generally monitored for unbalanced load. If the current exceeds a critical value, the circuit breakers are opened.

[redacted]

DTRA 3.3(b)(2),(8)

[redacted] OSD 3.3(b)(8)

[redacted]

DTRA 3.3(b)(2),(8)

REFERENCES

OSD 3.3(b)(8)

1. (U) N. J. Carron, and C. L. Longmire, *Magnetohydrodynamic EMP Environments*, MRC-R-724, Mission Research Corp., Santa Barbara, CA, September 1982 (Secret).
2. (U) P. Dyal, *Starfish Plasma Expansion*, AFWL-TR-66-74, March 1967 (Secret-RD).
3. (U) H. A. Bomke et al., *J. Geo. Phys. Res. 69*, 3125, (1964).
4. (U) C. W. Anderson, L. J. Lanzerotti, and C. C. Maclennan, "Outage of the L-4 System and the Geomagnetic Disturbances of 4 August 1972," *Bell Syst. Tech. J. 53*, 1817 (1974).
5. (U) J. G. Kappenman, V. D. Albertson, and N. Mohan, *Investigation of Geomagnetically Induced Currents in the Proposed Winnipeg-Duluth-Twin Cities 500 kV Transmission Line*, EPRI Report EL-1949, July 1981.

Additional References of Interest

(U) N. J. Carron, *A Model for MHDEMP From a High-Altitude Nuclear Burst*, MRC-R-658, Mission Research Corp., Santa Barbara, CA, January 1982 (Confidential).

(U) S. Chavin, W. F. Crevier, and R. W. Kilb, *MHDEMP of Starfish: 1 to 40 sec*, MRC-R-684, Mission Research Corp., Santa Barbara, CA, January 1982.

(U) S. Chavin, et al., *MHD EMP Code Simulation of Starfish*, MRC-R-516, Mission Research Corp., Santa Barbara, CA, August 1979.

(U) J. M. Harberger, R. Kilb, and C. L. Longmire, *Burst Region and Remote Current Sources Contributing to MHD-EMP*, MRC-R-264, DNA 4021T, Mission Research Corp., Santa Barbara, CA, May 1976 (Confidential-FRD).

(U) M. A. Messier and C. L. Longmire, *MHD EMP Effects on the L-4 Cable System*, MRC-N-156, DNA 3595T, October 1974 (Confidential).

(U) M. A. Messier, R. W. Kilb, and C. L. Longmire, *Magnetohydrodynamic EMP*, MRC-R-56, DNA 3510T, Mission Research Corp., Santa Barbara, CA, February 1973 (Confidential).